AMERICAN SOCIETY FOR MICROBIOLOGY | Applied and Environmental Microbiology®

BIODEGRADATION

Sterilizing Processes and Mechanisms for Treatment of *Escherichia coli* with Dielectric-Barrier Discharge Plasma

Hao Wang,[a] Liyang Zhang,[a] Haiyun Luo,[a] Xinxin Wang,[a] Jinfeng Tie,[b] Zhe Ren[b]

[a]Department of Electrical Engineering, Tsinghua University, Beijing, China
[b]PLA Center for Disease Prevention and Control, Beijing, China

ABSTRACT With increasing attention toward novel sterilization methods, plasma sterilization has gained more and more interest. However, the underlying mechanisms are still unknown. In this paper, we investigated the inactivation of *Escherichia coli* using dielectric-barrier discharge (DBD) plasma in saline water. There were three processes shown in the survival curve, namely, during the preparation period, the reaction period, and the saturation period. Observations under a transmission electron microscope (TEM) and detection by Fourier transform infrared spectroscopy (FT-IR) supplied adequate details regarding these processes. Based on these results, we infer that during the preparation period, the main process is the accumulation of chemical substances. During the reaction period, adequate amounts of chemicals decompose and denature cell membranes and macromolecules to kill bacteria in large quantities. During the saturation period, the killing effect decreases because of the protection by clustered cells and the saturation of pH. This study of sterilizing processes systematically reveals the mechanisms of plasma sterilization.

IMPORTANCE Compared with traditional methods, plasma sterilization has advantages of high efficiency, easy operation, and environmental protection. This may be more suitable for air and sewage sterilization in specific spaces, such as hospitals, laboratories, and pharmaceutical factories. However, the mechanisms of sterilization are still relatively unknown, especially for bactericidal activities. Knowledge of sterilization processes provides guidance for practical applications. For example, the bactericidal action mainly occurs during the reaction period, and the treatment time can be set based on the reaction period, which could save a lot of energy. The results of this study will help to improve the efficiency of plasma sterilization devices.

KEYWORDS processes, mechanisms, *Escherichia coli*, sterilization, DBD plasma

Bacterial decontamination plays an important role in medical facilities, industrial processing, food security, biosafety, and environmental applications (1–6). As a state-of-the-art method, plasma sterilization has attracted more and more attention for its high efficiency, easy operation, and environmental protection. Plasma is typically produced by applying high voltage to two electrodes until the gap gas is ionized. The plasma contains many ions, electrons, radicals, UV photons, and chemicals (7). These energetic particles can easily destroy biological structures or macromolecules for rapid sterilization. In practical applications, many researchers have designed efficient plasma generators to kill bacteria (8–12).

Plasma sterilization involves very complex physical, chemical, and biological processes. However, there is a lack of systematic research on the underlying mechanism(s). Researchers attempted to study the mechanism from separate aspects. Some researchers focused on UV radiation, free radicals, and metastable particles (13–15). Some researchers paid attention to the active chemicals (such as reactive nitrogen species [RNS], reactive oxygen species [ROS], etc.) produced by plasma in solution (16, 17).

Citation Wang H, Zhang L, Luo H, Wang X, Tie J, Ren Z. 2020. Sterilizing processes and mechanisms for treatment of *Escherichia coli* with dielectric-barrier discharge plasma. Appl Environ Microbiol 86:e01907-19. https://doi.org/10.1128/AEM.01907-19.

Editor Robert M. Kelly, North Carolina State University

Address correspondence to Haiyun Luo, lhy@tsinghua.edu.cn.

Received 23 August 2019
Accepted 13 October 2019
Accepted manuscript posted online 18 October 2019
Published 13 December 2019

Some researchers were concerned about the changes to biological structures or macromolecules (such as cell membrane, DNA, etc.) (18–21). Most of these studies focused on the causes and results rather than the processes; thus, it is hard to reflect on the overall mechanism(s). However, investigating the processes of plasma sterilization systematically could reveal these mechanisms.

Survival curves are key data that reflect commonalities in plasma sterilization processes. Several investigators have performed analyses and formed hypotheses about the mechanisms behind these curves, but few have verified their hypotheses by experiments. Many studies have reported different shapes of survival curves: single-slope curves (15, 22), two-slope survival curves (8, 23, 24), and multislope survival curves (8, 25–27). Kelly-Wintenberg et al. proposed a well-known hypothesis of the two-slope survival curve (28): during the first killing stage, active plasma species react with the outer membranes of the cells, leading to damaging alterations. After this process, the reactive species can quickly cause cell death and result in a rapid second stage. Moisan et al. proposed mechanisms for the three-slope survival curve in low-pressure plasma sterilization (29). However, these hypotheses need further experimental proof.

In this paper, the sterilizing processes and mechanisms behind the survival curve were confirmed by various detection methods and were analyzed in depth. We used nanosecond-pulse dielectric-barrier discharge (DBD) plasma to kill *Escherichia coli* in saline water as a case study. The survival curve was divided into three parts: preparation period, reaction period, and saturation period. The results show that the sterilization effect is not obvious during the preparation period, the reaction period is the main time for sterilization effect, and the sterilization effect reaches saturation during the saturation period. This study provides a sound theoretical basis and experimental examples for other forms of plasma inactivation.

RESULTS AND DISCUSSION

Nanosecond-pulsed plasma was used to decrease the thermal effect of discharge, and we used an infrared thermometer to record the highest temperature (28 to 30°C) of the entire process. Therefore, we can exclude the influence of temperature on sterilization. Because this experiment was to treat *E. coli* in saline water, the effect of particle impact can also be neglected. The dielectric constant of water is very large, and the voltage in water is very small. Therefore, the sterilization effect of the electric field is not considered. According to the literature (30), UV radiation in atmospheric pressure discharge is not the main factor, and so the sterilization effect of UV radiation is not considered. In this situation, the main functional species of atmospheric pressure sterilization are the chemical substances produced by plasma and bacterial fluid (31). Based on the survival curve of plasma sterilization, cell morphology, the pH changes, and macromolecules at different times will be discussed.

Survival curve. To prolong the treatment time in order to detect the products, we choose a relatively high concentration of bacterial solution (about 10^9 CFU/ml). The peak voltage was −21.01 kV, and the single pulse power was ~3 mJ. The discharge mode was filament discharge, as shown in Fig. 1B (32). In this case, sterilization can be achieved in 5 min. According to the survival curve shown in Fig. 2A, the process was divided into three periods. To quantitatively describe the decreasing rate of different periods, we calculated the microbial reduction factor by using the curve shown in Fig. 2A. The reduction factor rate of the first period was 0.84/min. The reduction factor rate of the second period was 4.72/min. The reduction factor rate of the third period was 1.92/min. A similar curve was also obtained with 2.3 pH nitric acid treatment, as shown in Fig. 2B.

1. Preparation period (0 to 1 min). The bactericidal rate is low. Plasma is formed in the air, and it takes some time for the active airborne agents to react with the bacterial solution. At this time, the concentration of active airborne agents begins to increase, and the agents then diffuse slowly into the liquid to kill *E. coli*.

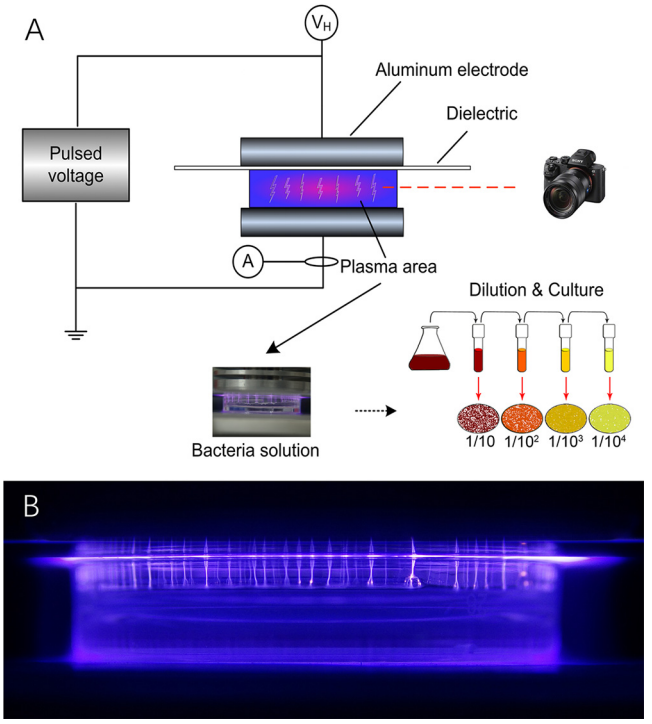

FIG 1 Schematic of plasma sterilization experiment (A) and image of plasma (B).

2. Reaction period (1 to 2 min). As the amount of active substances gradually increased in the water, a large number of bacteria died; thus, the killing speed becomes higher.
3. Saturation period (2 to 5 min). Since *E. coli* bacteria usually aggregate into clusters (this can be seen in the transmission electron microscope [TEM] images), the inner bacteria are surrounded by outer bacteria, making sterilization difficult. This phenomenon, mentioned in the literature, is called the long tail phenomenon (33). Combining the study results from the literature (31, 34, 35), we infer that active substances in plasma interact with the bacterial solution to produce ROS, RNS, and acids. These chemicals rupture and denature the cell membranes, cell walls, proteins, and genetic material (Fig. 3A). The basic processes of the plasma sterilization are established. We will next discuss the details of what happens in these processes.

Morphological analysis. In TEM imaging, the brightness of the image is related to the density of substances that the electrons pass through. Dense objects strongly

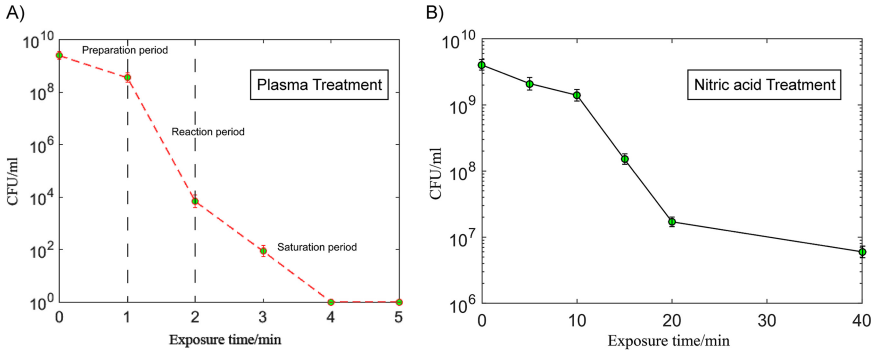

FIG 2 The survival curves of *E. coli* after plasma (A) and nitric acid (B) treatments.

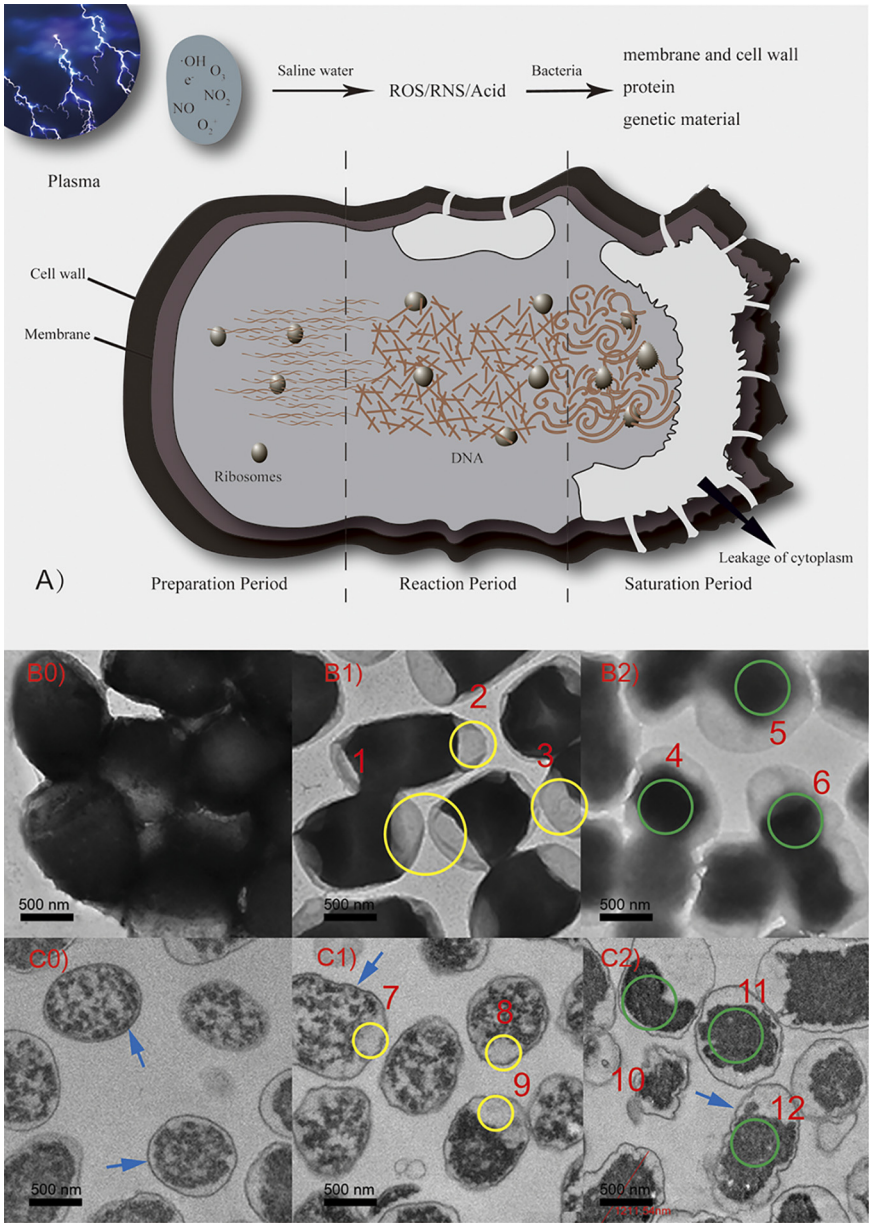

FIG 3 (A) Mechanism of plasma sterilization in different periods. (B0 to B2) TEM images of whole *E. coli* after treatment for 0, 1 min, or 2 min. (C0 to C2) TEM images of 70-nm sections of *E. coli* after treatment for 0, 1 min, or 2 min. Ruptures of *E. coli* membranes are highlighted by the yellow circles (1 to 3 and 7 to 9), and the denaturation of genetic material is highlighted by the green circles (4 to 6 and 10 to 12). The arrows point to the cell walls and membranes.

scatter electrons, shown as dark areas, whereas electrons pass directly through thin objects, shown as bright areas (electron transmission areas). The number of living bacteria mainly decreased by 5-log in first 2 min, and it was hard to analyze the TEM images from the last 3 min. Thus, we regard the control group, 1-min exposure group, and 2-min exposure group as the main research objects to explain the sterilization process. The overall mechanisms of plasma sterilization are shown in Fig. 3A and discussed in detail below.

First, during the preparation period (Fig. 3B0), the bacteria in the control group are plump and round. The normal *E. coli* cells have pressures of ~2 atm inside their membranes to maintain their shape (36). *E. coli* cells have capsules and mucous substances on their surfaces. Most of the structures are composed of lipopolysaccharide

complexes and proteins. The lipopolysaccharide complex enables bacteria to adhere to each other. The surfaces of living bacteria are sticky and facilitate agglomeration. In Fig. 3C0, the cell walls of *E. coli* cells appear smooth, the cell membranes are intact, the cytoplasm has not flowed out, and there are no electron transmission areas in the cells. The ribosomes are clearly visible and uniformly distributed. The main processes are that plasma interacts with saline water and that chemicals accumulate for the next period.

Second, after the 1-min treatment, the surface capsules of the dead *E. coli* cells have lost their bioactivity. The scattered and irregular distribution of the bacteria can be clearly seen in Fig. 3B1. The normal cell membrane is a protective membrane structure with a thickness of approximately 8 nm (36). If the cell membrane breaks down, the integrity of the cell is destroyed. The accumulated chemicals rupture the cell membranes, and the cytoplasm flows out, relieving the intracellular pressure. The edges of the cells begin to deform, and electron transmission areas appear at both ends. As shown in Fig. 3C1, the cell walls begin to deform in small areas. Cell membranes are ruptured and generate holes, resulting in the outflow of cytoplasm and some blank electron transmission areas at the end (yellow circles 1, 2, 3, 7, 8, and 9). Lipopolysaccharides are abundant on the cell walls of *E. coli* cells. The destruction and decomposition of these parts lead to some changes in the cell wall structure, but peptidoglycans are firmer and not easily destroyed. Thus, the cell wall maintains the basic morphology. The shapes of the ribosomes and genetic material remain unchanged, but the proteins begin to denature, as detected by Fourier transform infrared spectroscopy (FT-IR). Corresponding to the low killing rate during the first period, the results show that plasma destroys the cell walls and membranes and denatures the proteins in 0 to 1 min.

Third, after the 2-min treatment, as shown in Fig. 3B2, the entire cell membrane is destroyed and the cytoplasm flows out from all sides. The contrast between the cells and the background is reduced. Fig. 3C2 shows that the cell walls have been further destroyed, the external polysaccharides and proteins have been completely denatured, and the firm peptidoglycans maintained the cell morphology (blue arrows). The cells appear as deflated balls. The cell membranes are completely ruptured, and cytoplasm near the cell membranes has flowed out. The internal genetic material and ribosomes have begun to distort and tangle together to form more dense products. The dark areas shown in the picture are the denatured DNA fibers in the nucleus. Corresponding to the high killing rate during the second period, the results show that plasma treatment caused extensive destruction of lipopolysaccharides on the cell wall surfaces, overall destruction of cell membranes, and destruction of intracellular genetic material in 1 to 2 min.

Chemical measurements. We measured the three most relevant factors, the concentrations of H_2O_2 and NO_3^- and pH values, at different exposure times. The concentration of H_2O_2 remained at approximately 0.1 mmol/liter for 1 to 5 min. The pH decreases gradually over time, as shown in Fig. 4A. Figure 4B shows that the concentration of NO_3^- increases proportionally with treatment time. Compared with the other two chemical curves, the pH curve reflects the sterilization process appropriately. Other researchers reported that the background acidic solution is good for plasma sterilization and related to many bactericidal reactions (37). In the *E. coli* experiment, energetic electrons produced by plasma dissociate the bond of N_2. Moreover, the outcomes (NO and NO_2) combine with H_2O and produce nitric acid. These result in the decrease of pH value (37). Measurements of pH detector revealed that the pH value of the *E. coli* liquid decreased from 7 to 2.3 after plasma treatment. In Fig. 4A, we show the changes to pH values measured at different power levels. The three periods of pH change and sterilization are discussed as follows.

First, at 0 to 1 min (preparation period), the rate of pH value change was the highest. This corresponds to the first period of the bactericidal curve, indicating that the chemicals (NO and NO_2) react with water in the first minute to reduce the pH value. During this period, active substances in the air react with the solution and interact with the cell wall and cell membrane. The germicidal effect is relatively slow, but this lays the

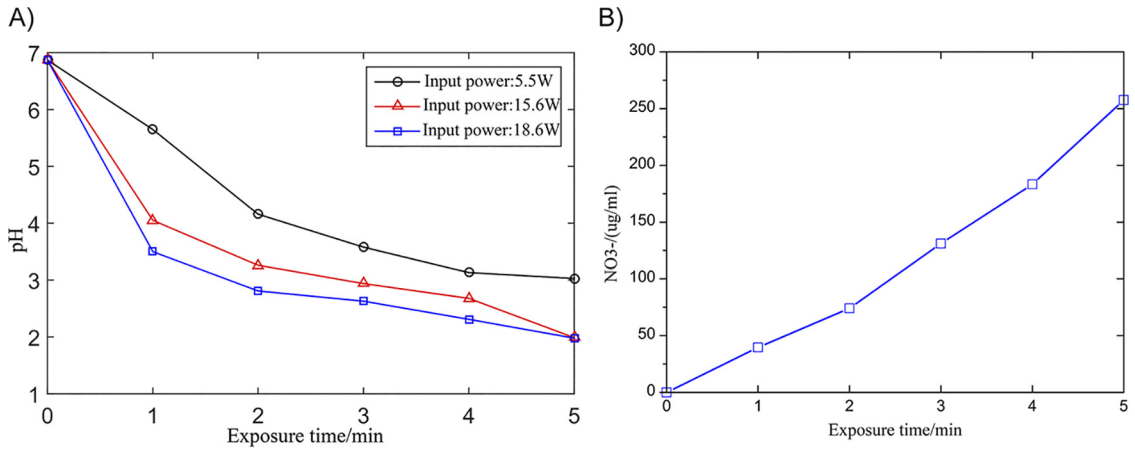

FIG 4 (A) pH values of bacterial solution at different input powers. (B) Concentrations of NO_3^- in the solution.

foundation for accelerated death in the second minute as a preparatory stage for bactericidal treatment.

Second, at 1 to 2 min (reaction period), the rate of pH decline was lower. This is because the plasma area in the petri dish is closed. With plasma treatment, the pH decreases gradually. At this stage, the acid produced by plasma discharge has gradually become saturated, but the nitrate concentration still increases. At this time, a large number of active substances can enter the cell membrane and be completely destroyed to complete large-scale killing. This is the most important process of plasma sterilization. It corresponds to the second part of the bactericidal curve.

Third, at 2 to 5 min, the oxidation of nitrogen continues; however, further acidification of the solution is hindered. This reflects the saturation of the interaction between plasma and the bacterial solution. The nitrate concentration continues to increase; however, the killing effect cannot be further increased. Corresponding to the third part of the sterilization curve, most of the *E. coli* cells are killed. Only a small proportion of the bacteria enclosed in the colonies require prolonged treatment for sterilization.

These results show that acid provides a good background for inactivation. In addition, we designed a comparative experiment to show that acids alone do not work very well for sterilization. Nitric acid at pH 2.3 was used to kill *E. coli*, and a survival curve similar to that for plasma sterilization was obtained. The sterilization curve is as shown in Fig. 2B. Although the treatment time was 10 times longer, the linearity of the sterilization curve is basically consistent with our plasma sterilization curve, which is also divided into three sections. Therefore, we infer that the plasma sterilization process is similar to that for nitric acid sterilization. From the above-described experimental results, we infer that the acid produced by DBD plasma can play a certain role and that plasma treatment is the superposition of several similar factors.

FT-IR analysis. FT-IR can provide direct information about bond order, electrostatic interactions, hydrogen bonds, charge distribution, protonation state, redox state, and kinetics. FT-IR detects infrared absorption peaks corresponding to different chemical bonds. By detecting the changes in different absorption peaks, we can assess the changes in cell macromolecules. The corresponding relationships between different wave numbers and substances are listed in Table 1 (38). A change in the absorbance amplitude indicates a change of content, and a shift in the peak indicates the denaturation of a substance. Among them, 3,283 cm^{-1} corresponds to N-H stretching of amide A in proteins, 2,918.13 cm^{-1}, 2,927.78 cm^{-1}, and 2,929.70 cm^{-1} correspond to the fat chains on the cell membrane, and 1,642 cm^{-1} and 1,542 cm^{-1} correspond to amide I and amide II protein bands, respectively. The peaks representing cell membrane structure and protein structure can be seen from the graph in Fig. 5. The treatment process is discussed as follows.

TABLE 1 FT-IR band assignments of *E. coli*

Wave no. (cm^{-1})	Functional group assignment
~3,200	N-H stretching of amide A in proteins
2,955–2,850	C-H asymmetric stretching of $-CH_2$ and $-CH_3$ in fatty acids
~1,637	Amide I of beta-pleated sheet structures of proteins
1,550–1,520	Amide II band of proteins
1,468	C-H deformation of CH_2 in lipids
1,415	C-O-H in plane bending in carbohydrates, DNA/RNA backbone, proteins
~1,400	C=O symmetric stretching of COO^- group in amino acids, fatty acids
~1,355	Wagging vibrations of methylene fragments
1,310–1,240	Amide band III components of proteins
1,250–1,225	P=O stretching asymmetric of PO_2^- phosphodiesters in phospholipids
1,084	Stretching P=O of phosphodiester, phosphorylated proteins, or polyphosphate products
900–600	Fingerprint region

First, during the preparation period (0 to 1 min), the absorbance of amide A decreased, the fat chain remained almost unchanged, and the protein was obviously influenced. The two peaks on the graph correspond to the secondary structure of the protein. This means that the protein has been modified. This is consistent with the destruction of the cell wall membrane observed by transmission electron microscopy. At this time, polysaccharides and proteins on cell walls are destroyed; a large number of chemical substances can destroy the cell membrane. Many holes are produced in the cell membrane and cytoplasm flows out.

Second, during the reaction period (1 to 2 min), amide A decreased sharply, the fat chain content decreased, the denaturation of protein was severest, and the amino acids and fatty acids remained unchanged. Carbohydrates, proteins, DNA, and so on undergo tremendous changes, at which time the cell death rate is the highest.

Third, during the saturation period (2 to 5 min), amide A and adipose chains on cell membranes remained almost unchanged. Protein was no longer significantly modified. The bactericidal process was basically completed, and the few surviving bacteria were being killed. A new peak appeared at 1,355 cm^{-1}. This absorption is ascribed to the

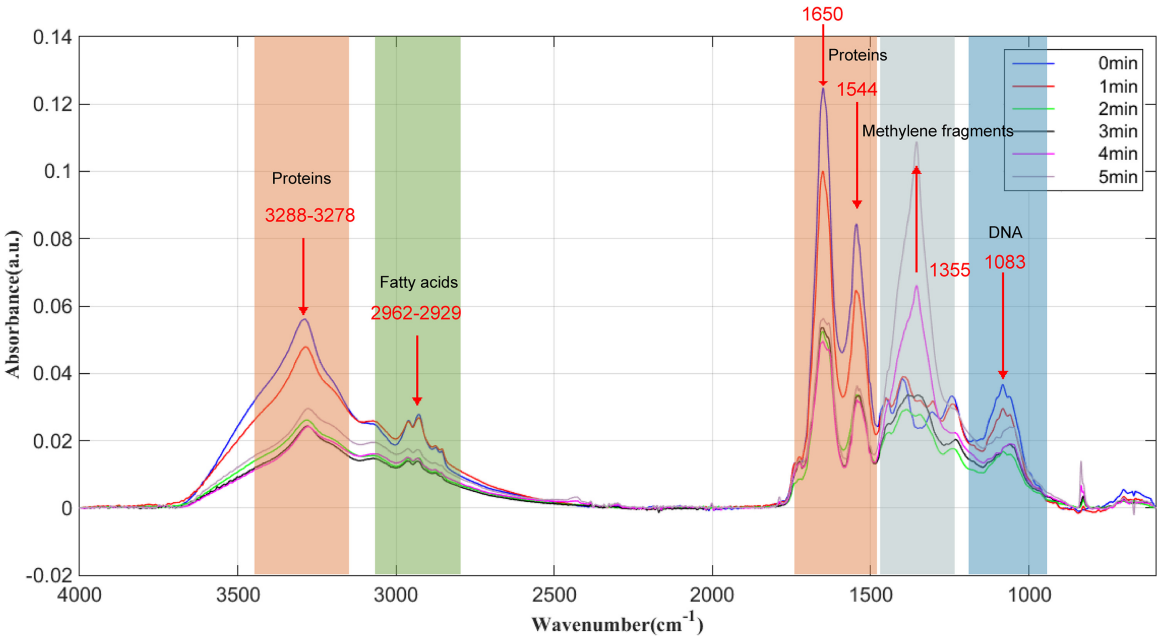

FIG 5 FT-IR of *E. coli* after baseline correction at different treatment times.

wagging vibrations of methylene fragments (39). It indicates that methylene fragments are the main by-products.

Conclusions. In this paper, a complete plasma sterilization process is established by studying the plasma sterilization curve and combining the observation results from TEM, pH detection, and analysis of FT-IR. The process is divided into three stages: the preparation period, reaction period, and saturation period.

First, during the preparation period (0 to 1 min), the reaction between plasma and water results in an accumulation of a large number of chemical substances. The pH value declines rapidly, and the rate of bacterial death is low. In this process, polysaccharides outside the cell walls are decomposed, the cell membranes are partially destroyed, a portion of the cytoplasm is released, genetic material in the cells remains basically unchanged, and the secondary structures of proteins begin to degenerate.

Second, during the reaction period (1 to 2 min), a large number of chemical substances begin to interact with cells. Bacteria die in large quantities. It is the main functional time of sterilization. The decline in pH values slows. The cell walls and cell membranes are completely destroyed. The cytoplasm is exuded in large quantities. Proteins are completely denatured. The genetic material in cells is also destroyed.

Third, during the saturation period (2 to 5 min), the killing rate of *E. coli* declines in this final stage because the aggregated bacteria protect those that are within the clusters. The pH of the solution has reached saturation. The phosphorus organic compounds forming cell membranes are decomposed into phosphate.

This research explains the processes by which plasma sterilizes bacteria, provides a basis for the further study of the sterilization mechanism, and provides theoretical support for plasma sterilization technology.

MATERIALS AND METHODS

Bacterial selection. We selected *Escherichia coli* ATCC 15597 as the test organism. Current research of the disinfection, cell morphology, and FT-IR of *E. coli* is relatively mature and complete (40).

Plasma reactor. We established a DBD generator with pulse power to produce plasma. The pulse power source we selected was a nanosecond-pulse generator based on semiconductor opening switches (SOS) (41), for which the parameters were 44-kV peak-to-peak voltage, 300-ns pulse rise time, 250-ns pulse width, and 600-Hz pulse repetition frequency.

The diameter of high-voltage electrodes and the grounded electrode, made from cylindrical aluminum, was 5 cm. In the horizontal direction of discharge, we put a camera to photograph the discharge. The petri dish containing 2 ml bacterial liquid was placed in the 10-mm gap. To avoid the discharge developing into arc plasma, we used 1-mm quartz as the dielectric barrier material. Figure 1B shows that the discharge starts along the inner wall of the petri dish. When the applied voltage increases, many bright filament discharges occur in the entire space. These filaments are produced in the air, and the active substances permeate into the liquid to inactive *E. coli* cells.

The current and voltage were displayed on a LeCroy 610zi digital oscilloscope. To prevent electromagnetic interference, an isolation transformer was used to isolate the discharge power supply.

Plasma experiments. The bacterial liquid contained *E. coli* (initial concentration of $\sim 10^9$ CFU/ml) in 2 ml 0.9% saline water (pH 7). We prepared 6 groups of bacterial liquid in petri dishes and set the parameter of plasma discharge. The bacteria were placed in the center of the gas gap and the power was turned on. The *E. coli* cells were exposed for 0 min, 1 min, 2 min, 3 min, 4 min, and 5 min. After treatment, we determined the pH and scanned the bacterial solution by FT-IR. Then, the bacterial liquid was serially diluted 10-fold in sterile ultrapure water and inoculated into agar medium; CFU were counted after incubating at 37°C for 24 h. Subsamples were observed under a TEM to capture the changes of the morphology and with FT-IR after different treat times.

Nitric acid treatment. One milliliter nitric acid (pH 1.98) was mixed with 1 ml bacterial solution in normal saline. The pH of the mixed solution was kept at 2.3 for more than 40 min. After treatment, 0.01 mmol/liter of phosphate-buffered saline (PBS) was used to stop the inactivation.

Transmission electron microscopy. A TEM provides more detail of bacteria than a scanning electron microscope. In this experiment, we adopted two methods for TEM photography. The first is an observation of the entire bacterium without slicing. This method can save a lot of slicing pretreatment time. The observation results show the outline and perspective of the whole bacterium. The other method is TEM observation after slicing. The advantage of this method is that the cell membrane boundaries and cytoplasm can be clearly observed. An FEI Tecnai Spirit TEM D1266 was used to capture images of *E. coli* morphology. A Leica UC7+FC7 microtome was used to obtain 70-nm slices of *E. coli* cells.

Measurement of pH. The pH value of the bacterial solution was measured by a Seven2Go pH meter after plasma treatment. The range of detection is −2.00 to 20.00, the resolution is 0.01.

Measurement of nitrate. The concentration of nitrate was detected by Metrohm 761 Compact ion chromatography. The relative standard deviation is less than 0.5%. The detection limit is parts per billion to parts per million.

Measurement of H_2O_2. The concentration of H_2O_2 was detected by the iodometric method (42) and a Bio-Rad IQ5 UV spectrophotometer.

FT-IR. The FT-IR spectrometer used in this experiment was produced by PE Company. The range of spectrum scanning is 4,000 to 600 cm^{-1} and the resolution is 4 cm^{-1}. The software can compensate for the interference of CO_2 and H_2O in the air. The changes of macromolecules before and after treatment were detected by FT-IR. FT-IR can provide direct information about the bond level, electrostatic interactions, hydrogen bonds, charge distribution, protonation, and redox state and dynamics and reflect molecular vibration information of proteins, polysaccharides, lipids, nucleic acids, and other biological macromolecules in microbial cytoplasm, cell membranes, cell walls, or nuclei. The advantage of this method is that the overall changes resulting from the plasma sterilization process can be analyzed.

Statistical analysis. All experiments were performed independently at least three times. Statistical analyses were performed in Origin8.5.1 (OriginLab Corporation, Northampton, MA, USA) using analyses of variance (ANOVAs) with Fisher's least significant difference (LSD); the significance level was set at a P value of ≤ 0.05.

ACKNOWLEDGMENTS

This research was support by National Key R&D Program of China (2017YFC1200404).

REFERENCES

1. Mandal R, Singh A, Singh AP. 2018. Recent developments in cold plasma decontamination technology in the food industry. Trends Food Sci Technol 80:93–103. https://doi.org/10.1016/j.tifs.2018.07.014.
2. Hayashi N, Goto M, Itarashiki T, Yonesu A, Sakudo A. 2018. Current plasma sterilization and disinfection studies. J Photopolym Sci Technol 31:389–398. https://doi.org/10.2494/photopolymer.31.389.
3. Fridman G, Friedman G, Gutsol A, Shekhter AB, Vasilets VN, Fridman A. 2008. Applied plasma medicine. Plasma Process Polym 5:503–533. https://doi.org/10.1002/ppap.200700154.
4. Mir SA, Shah MA, Mir MM. 2016. Understanding the role of plasma technology in food industry. Food Bioprocess Technol 9:734–750. https://doi.org/10.1007/s11947-016-1699-9.
5. Thirumdas R, Sarangapani C, Annapure US. 2015. Cold plasma: a novel non-thermal technology for food processing. Food Biophys 10:1–11. https://doi.org/10.1007/s11483-014-9382-z.
6. Scholtz V, Pazlarova J, Souskova H, Khun J, Julak J. 2015. Nonthermal plasma–a tool for decontamination and disinfection. Biotechnol Adv 33:1108–1119. https://doi.org/10.1016/j.biotechadv.2015.01.002.
7. Chen FF. 1984. Introduction to plasma physics and controlled fusion, 2nd ed. Springer, Cham, Switzerland. https://doi.org/10.1007/978-3-319-22309-4.
8. Dasan BG, Mutlu M, Boyaci IH. 2016. Decontamination of *Aspergillus flavus* and *Aspergillus parasiticus* spores on hazelnuts via atmospheric pressure fluidized bed plasma reactor. Int J Food Microbiol 216:50–59. https://doi.org/10.1016/j.ijfoodmicro.2015.09.006.
9. Xu ZM, Shen J, Zhang ZL, Ma J, Ma RH, Zhao Y, Sun Q, Qian SL, Zhang H, Ding LL, Cheng C, Chu PK, Xia WD. 2015. Inactivation effects of non-thermal atmospheric-pressure helium plasma jet on Staphylococcus aureus biofilms. Plasma Process Polym 12:827–835. https://doi.org/10.1002/ppap.201500006.
10. Shen J, Cheng C, Fang SD, Xie HB, Lan Y, Ni GH, Meng YD, Luo JR, Wang XK. 2012. Sterilization of *Bacillus subtilis* spores using an atmospheric plasma jet with argon and oxygen mixture gas. Appl Phys Express 5:036201. https://doi.org/10.1143/APEX.5.036201.
11. Liang Y, Wu Y, Sun K, Chen Q, Shen F, Zhang J, Yao M, Zhu T, Fang J. 2012. Rapid inactivation of biological species in the air using atmospheric pressure nonthermal plasma. Environ Sci Technol 46:3360–3368. https://doi.org/10.1021/es203770q.
12. Klämpfl TG, Isbary G, Shimizu T, Li Y-F, Zimmermann JL, Stolz W, Schlegel J, Morfill GE, Schmidt H-U. 2012. Cold atmospheric air plasma sterilization against spores and other microorganisms of clinical interest. Appl Environ Microbiol 78:5077–5082. https://doi.org/10.1128/AEM.00583-12.
13. Ma RN, Wang GM, Tian Y, Wang KL, Zhang JE, Fang J. 2015. Non-thermal plasma-activated water inactivation of food-borne pathogen on fresh produce. J Hazard Mater 300:643–651. https://doi.org/10.1016/j.jhazmat.2015.07.061.
14. Yonemori S, Ono R. 2014. Flux of OH and O radicals onto a surface by an atmospheric-pressure helium plasma jet measured by laser-induced fluorescence. J Phys D Appl Phys 47:125401. https://doi.org/10.1088/0022-3727/47/12/125401.
15. Sysolyatina E, Mukhachev A, Yurova M, Grushin M, Karalnik V, Petryakov A, Trushkin N, Ermolaeva S, Akishev Y. 2014. Role of the charged particles in bacteria inactivation by plasma of a positive and negative corona in ambient air. Plasma Process Polym 11:315–334. https://doi.org/10.1002/ppap.201300041.
16. Schnabel U, Andrasch M, Weltmann KD, Ehlbeck J. 2014. Inactivation of vegetative microorganisms and *Bacillus atrophaeus* endospores by reactive nitrogen species (RNS). Plasma Process Polym 11:110–116. https://doi.org/10.1002/ppap.201300072.
17. Vandamme M, Robert E, Lerondel S, Sarron V, Ries D, Dozias S, Sobilo J, Gosset D, Kieda C, Legrain B, Pouvesle JM, Le Pape A. 2012. ROS implication in a new antitumor strategy based on non-thermal plasma. Int J Cancer 130:2185–2194. https://doi.org/10.1002/ijc.26252.
18. Zhang H, Ma J, Shen J, Lan Y, Ding LL, Qian SL, Xia WD, Cheng C, Chu PK. 2018. Roles of membrane protein damage and intracellular protein damage in death of bacteria induced by atmospheric-pressure air discharge plasmas. RSC Adv 8:21139–21149. https://doi.org/10.1039/C8RA01882K.
19. Sakudo A, Miyagi H, Horikawa T, Yamashiro R, Misawa T. 2018. Treatment of *Helicobacter pylori* with dielectric barrier discharge plasma causes UV induced damage to genomic DNA leading to cell death. Chemosphere 200:366–372. https://doi.org/10.1016/j.chemosphere.2018.02.115.
20. Boehm D, Heslin C, Cullen PJ, Bourke P. 2016. Cytotoxic and mutagenic potential of solutions exposed to cold atmospheric plasma. Sci Rep 6:21464. https://doi.org/10.1038/srep21464.
21. Arjunan KP, Sharma VK, Ptasinska S. 2015. Effects of atmospheric pressure plasmas on isolated and cellular DNA-a review. Int J Mol Sci 16:2971–3016. https://doi.org/10.3390/ijms16022971.
22. Choi JH, Han I, Baik HK, Lee MH, Han DW, Park JC, Lee IS, Song KM, Lim YS. 2006. Analysis of sterilization effect by pulsed dielectric barrier discharge. J Electrostat 64:17–22. https://doi.org/10.1016/j.elstat.2005.04.001.
23. Ziuzina D, Patil S, Cullen PJ, Keener KM, Bourke P. 2014. Atmospheric cold plasma inactivation of *Escherichia coli*, *Salmonella enterica* serovar Typhimurium and *Listeria monocytogenes* inoculated on fresh produce. Food Microbiol 42:109–116. https://doi.org/10.1016/j.fm.2014.02.007.
24. Schnabel U, Niquet R, Krohmann U, Winter J, Schluter O, Weltmann KD, Ehlbeck J. 2012. Decontamination of microbiologically contaminated specimen by direct and indirect plasma treatment. Plasma Processes Polym 9:569–575. https://doi.org/10.1002/ppap.201100088.
25. Singh RK, Babu V, Philip L, Ramanujam S. 2017. Disinfection of water using pulsed power technique: effect of system parameters and kinetic study, p 307–336. *In* Babu GLS, Saride S, Basha BM (ed), Sustainability

issues in civil engineering. Springer, Singapore. https://doi.org/10.1007/978-981-10-1930-2_17.
26. Yannam SK, Estifaee P, Rogers S, Thagard SM. 2018. Application of high voltage electrical discharge plasma for the inactivation of *Escherichia coli* ATCC 700891 in tangerine juice. Lebenson Wiss Technol 90:180–185. https://doi.org/10.1016/j.lwt.2017.12.018.
27. Santos LCO, Cubas ALV, Moecke EHS, Ribeiro DHB, Amante ER. 2018. Use of cold plasma to inactivate *Escherichia coli* and physicochemical evaluation in pumpkin puree. J Food Prot 81:1897–1905. https://doi.org/10.4315/0362-028X.JFP-18-136.
28. Kelly-Wintenberg K, Montie TC, Brickman C, Roth JR, Carr AK, Sorge K, Wadsworth LC, Tsai P. 1998. Room temperature sterilization of surfaces and fabrics with a one atmosphere uniform glow discharge plasma. J Ind Microbiol Biotechnol 20:69–74. https://doi.org/10.1038/sj.jim.2900482.
29. Moisan M, Barbeau J, Crevier MC, Pelletier J, Philip N, Saoudi B. 2002. Plasma sterilization. Methods and mechanisms. Pure Appl Chem 74:349–358. https://doi.org/10.1351/pac200274030349.
30. Dobrynin D, Friedman G, Fridman A, Starikovskiy A. 2011. Inactivation of bacteria using dc corona discharge: role of ions and humidity. New J Phys 13:103033. https://doi.org/10.1088/1367-2630/13/10/103033.
31. Zhou RW, Zhou RS, Prasad K, Fang Z, Speight R, Bazaka K, Ostrikov K. 2018. Cold atmospheric plasma activated water as a prospective disinfectant: the crucial role of peroxynitrite. Green Chem 20:5276. https://doi.org/10.1039/C8GC02800A.
32. Luo H, Liu K, Ran J, Yue Y, Wang X, Yap S, Wong C. 2014 Study of dielectric barrier Townsend discharge in 3-mm air gap at atmospheric pressure. IEEE Trans Plasma Sci IEEE Nucl Plasma Sci Soc 42:1211–1215. https://doi.org/10.1109/TPS.2014.2312543.
33. Shintani H, Sakudo A, Burke P, McDonnell G. 2010. Gas plasma sterilization of microorganisms and mechanisms of action (review). Exp Ther Med 1:731–738. https://doi.org/10.3892/etm.2010.136.
34. Pai K, Timmons C, Roehm KD, Ngo A, Narayanan SS, Ramachandran A, Jacob JD, Ma LM, Madihally SV. 2018. Investigation of the roles of plasma species generated by surface dielectric barrier discharge. Sci Rep 8:16674. https://doi.org/10.1038/s41598-018-35166-0.
35. Hertwig C, Meneses N, Mathys A. 2018. Cold atmospheric pressure plasma and low energy electron beam as alternative nonthermal decontamination technologies for dry food surfaces: a review. Trends Food Sci Technol 77:131–142. https://doi.org/10.1016/j.tifs.2018.05.011.
36. Madigan MT, Martinko JM, Brock TD, Parker J. 2000. Brock biology of microorganisms. 9th ed. Prentice Hall, Upper Saddle River, NJ.
37. Yokoyama T, Ikawa S, Kitano K. 2019. Plasma disinfection via the reduced-pH method using an *ex vivo* porcine contaminated skin model. J Phys D Appl Phys 52:265401. https://doi.org/10.1088/1361-6463/ab1740.
38. Khan MSI, Lee EJ, Kim Y. 2016. A submerged dielectric barrier discharge plasma inactivation mechanism of biofilms produced by *Escherichia coli* O157:H7, *Cronobacter sakazakii*, and *Staphylococcus aureus*. Sci Rep 6:37072. https://doi.org/10.1038/srep37072.
39. Cieślik-Boczula K, Czarnik-Matusewicz B, Perevozkina M, Filarowski A, Boens N, Borggraeve WMD, Koll A. 2008. ATR-IR spectroscopic study of the structural changes in the hydrophobic region of ICPAN/DPPC bilayers. J Mol Struct 878:162–168. https://doi.org/10.1016/j.molstruc.2007.08.003.
40. Neidhardt FC, Ingraham JL, Low KB, Magasanik B, Schaechter M, Umbarger HE (ed). 1987. Escherichia coli and Salmonella typhimurium: cellular and molecular biology, vol I and II. ASM Press, Washington DC.
41. Jiang W, Yatsui K, Takayama K, Akemoto M, Nakamura E, Shimizu N, Tokuchi A, Rukin S, Tarasenko V, Panchenko A. 2004 Compact solid-state switched pulsed power and its applications. Proc IEEE Inst Electr Electron Eng 92:1180–1196. https://doi.org/10.1109/jproc.2004.829003.
42. De Laat J, Gallard H. 1999 Catalytic decomposition of hydrogen peroxide by Fe(III) in homogeneous aqueous solution: mechanism and kinetic modeling. Environ Sci Technol 33:2726–2732. https://doi.org/10.1021/es981171v.